From the work of
Comité Européen du Béton

Title No. 57-1

Researches Toward a General Flexural Theory for Structural Concrete

By HUBERT RÜSCH

This paper is directed toward formulation of a general flexural theory based on a careful study of all important factors regarding the properties of concrete. The fact that strength and deformation of concrete depend on time is considered. The theory is based on recent tests permitting determination of the behavior of the compression zone in flexure for continuous load increase at different strain rates, and for constant sustained load. Having derived stress-strain relationships for these various types of loading, other factors were studied systematically, such as effect of concrete strength, position of neutral axis, and shape of cross section. The general theory developed is primarily a study of the true behavior of structural members. Since simplified assumptions are avoided, it naturally does not lead to simple formulas such as are desired for structural design. The theory fulfills the important function of furnishing a reliable method for the evaluation of simplified design formulas. It is also possible, however, to present all new concepts and results of this theory in the form of a simple diagram which can be used for the solution of design problems for selected cross sections ranging from pure bending to pure compression, regardless of concrete quality and the type of steel used, and independent of whether prestressing is applied or not.

■ RESEARCH IN THE STRUCTURAL CONCRETE FIELD is faced today with problems of unusual challenge. We find ourselves in a period of change characterized by the abandonment of the elastic theory in favor of the plastic theory, and by a conversion from allowable stresses as a basis of design to ultimate strength design. Although these trends have persisted for some time, the new methods are finding slow acceptance among design engineers in some countries. This is probably at least in part due to the fact that structural engineering can look back on a thousand-year tradition, and this tradition is by its nature a conservative one. Another reason of equal importance is the lack of detailed and extensive knowledge regarding the properties of materials desirable in the development and introduction of new methods.

In recent decades, progress has been made toward replacing structural design methods disregarding plastic properties of materials by

ACI member **Hubert Rusch** has been, since 1945, a professor and director of the Engineering Materials Laboratory, Technical University, Munich, Germany. Dr. Rusch has won much prominence in Europe and South America through his design and construction of outstanding reinforced concrete structures. He has played an active part in reinforced concrete research, and in the development of shell structures (for which he received the Longstreth Medal prior to World War II), prestressed concrete, and precast construction.

new ones, which represent actual conditions to a greater degree. Numerous investigations of structural concrete have been conducted leading to several new design theories which generally are in good agreement with test results in the case of pure flexure. However, these theories start from very different, sometimes even contradictory, assumptions about the physical behavior of the component materials. This is probably a major reason why none of the new methods has found world-wide acceptance. An engineer seeks to analyze the true behavior of structures. He cannot be convinced by approximately correct results obtained on the basis of widely different assumptions. The agreement between the results of various theories in design, however, is not at all surprising since only the case of under-reinforced beams has often been cited in comparisons with test data. The tensile force in the steel at failure is determined entirely by the yield point; the lever arm of the internal forces is insensitive to assumptions regarding concrete stress. Only tests of over-reinforced members can furnish a true measure of the validity of a flexural theory. There is a need for a theory which is not restricted to approximate results in a limited range. Such a theory must be based on the actual properties of the materials and must be valid for all cases of loading, from pure bending to pure compression.

The reason why authors differ so widely in appraising the physical behavior of concrete in flexure probably lies in the fact that their knowledge is based almost entirely on beam tests. Only three conditions are available for the evaluation of such tests: the equilibrium condition, the deformation condition, and Bernouilli's assumption of plane sections remaining plane. As the number of unknowns is generally greater than the number of equations, some plausible assumptions must be made in the evaluation of certain quantities. As the required quantities are closely interrelated, it is quite understandable that one may thus arrive at widely different solutions.

It is only lately that attempts were made to establish the needed relationships in a direct manner. First among these should be mentioned tests on centrally and eccentrically loaded prisms conducted by Hognestad,[1,2] Moenaert,[3] and Rüsch,[4] which led to an extensive clarification of the behavior of the compression zone in flexure under *short-time* load only.

However, strength decreases under the action of *sustained loads.* Creep of the concrete leads to an increase in concrete strain in the extreme compressive fiber. This results in a lower neutral axis and a reduction of the lever arm of the internal forces. Consequently, the stress in the reinforcement becomes higher. A more important consideration is the reduction of concrete strength under the action of sustained load. This problem has been studied in detail only in recent years.

The following discussion reports results of new tests whose objective was to study effects of time such as age of concrete and duration of loading. These tests constitute the basis of the new flexural theory.

Notation

Notation is defined in Fig. 1 and frequently also in the text. In addition, some frequently used symbols are:

A_c = area of concrete compression zone (for symmetrical bending of a rectangular cross section, $A_c = bc$)

α = stress block factor = $C/A_c f_c' = f_{avg}/f_c'$

$c_{(a+t)}$, c_t, c_λ = coefficients defined by Eq. (2)

f_{avg} = average stress in concrete compression zone at ultimate strength

f_c = concrete stress

f_c' = concrete cylinder strength

f'_{c28} = 28-day cylinder strength

$f'_{c\,(a+t)}$ = strength of concrete failing under sustained load at the time t days after loading at an age of a days

f_{su} = stress in tensile steel at ultimate strength of reinforced concrete member

f'_{su} = stress in compression steel at ultimate strength of reinforced concrete member

k_u = ratio c/d at ultimate strength, Fig. 1

j_u = value of j at ultimate strength, Fig. 1

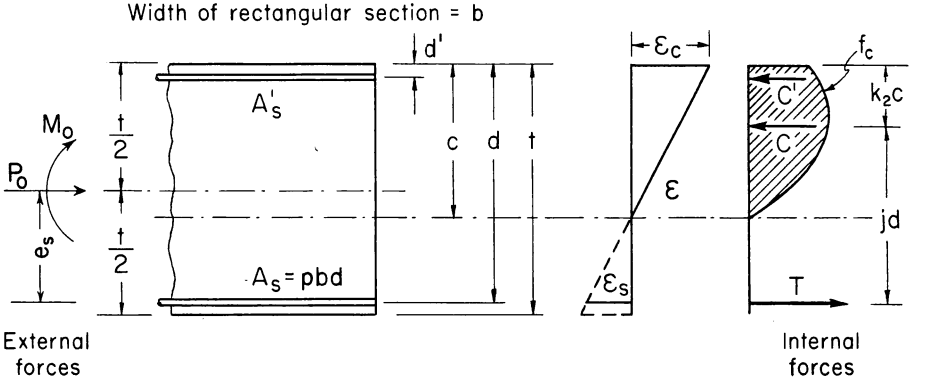

Fig. 1—Notation

M = moment of internal concrete force about centroid of tensile reinforcement; at ultimate strength $M = M_u$

m = relative internal resisting moment of concrete compression zone defined by Eq. (1), at ultimate strength $m = m_u$

M_o = moment of external forces with respect to centroid of cross section

P_o = external axial force acting in the centroid of cross section

e_s = distance between centroid of tensile reinforcement and centroid of cross-section (for symmetric loading of rectangular section $e_s = d - t/2$)

ε = concrete strain

ε_c = concrete strain in extreme fiber

ε_u = concrete strain in extreme fiber at ultimate strength

ε_s = tensile strain in reinforcement

ε_{su} = tensile strain in reinforcement at ultimate strength

RATE OF LOADING EFFECTS

Standards of some countries require that in tests of materials the load be applied at a certain constant rate. However, this requirement cannot be satisfied at high loads for materials exhibiting an elasto-plastic behavior. For example, in testing steel in the yield range, the rate of deformation would become extremely high. Even if our testing machines could satisfy this requirement, such testing would still have to be ruled out because it leads to completely misleading results.

The above-mentioned requirement has another disadvantage. Under constant rate of loading, the stress-strain diagram can be recorded only up to a maximum stress, after which further load increase is no longer possible. In this study, we wish to examine the portion of the stress-strain curve beyond maximum stress, since it has a considerable effect on the stresses produced in a concrete structure.

For these reasons, the requirement contained in some standards specifying a constant rate of loading must be modified for research purposes. It should be replaced by a more rational requirement, namely that all tests of materials be carried out under constant rate of strain. One can then determine the descending portion of the stress-strain curve as the deformation continues to increase further under decreasing load after the maximum stress is reached.

With increasing duration of loading, as mentioned earlier, strength drops and deformation increases. Hence, the magnitude of the selected rate of strain has a strong effect on the shape of the stress-strain curve. This was specially pointed out by Rasch[5] who studied this effect on three different quality classes of concrete at strain rates from 0.001 per min to 0.001 per 70 days under concentric load in the Munich Materials Laboratory.

In carrying out these tests the compressive force was regulated manually in such a way that strain increased at the desired constant rate. Due to the heterogeneous nature of concrete, strain under a

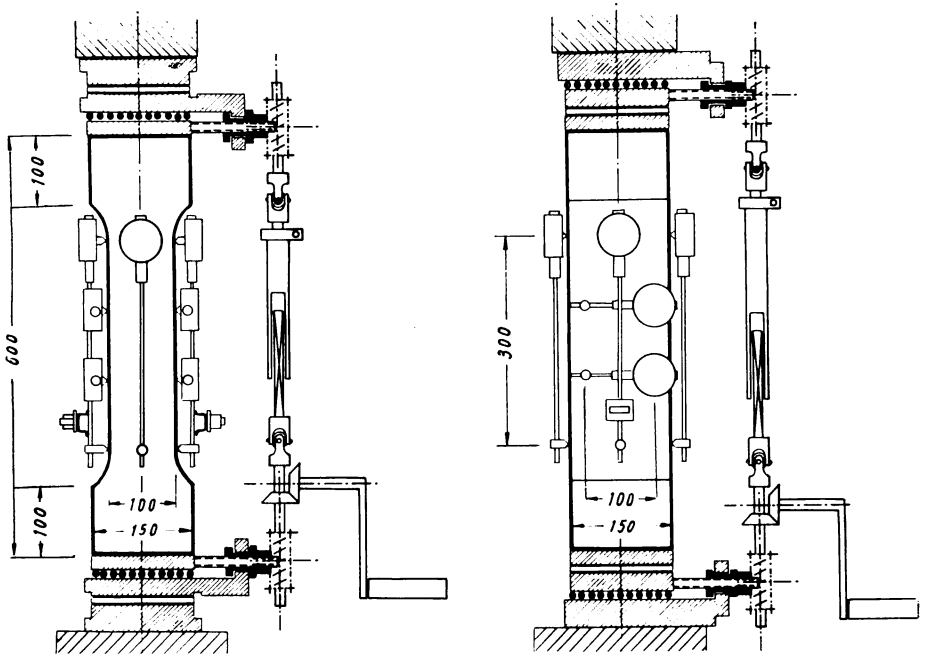

Fig. 2—Test arrangement and centering device (dimensions in millimeters). Left—Front view. Right—Side view

concentrically applied load is not necessarily the same on all sides of the test specimen. To eliminate this effect, the centering device shown in Fig. 2 was built into the testing machine to permit lateral displacement of the loaded test specimen in two directions with respect to the force axis. At all load levels, the position of the specimen was so adjusted by lateral displacements that strain on all four sides of the specimen at midheight remained equal. Such manual regulation becomes difficult at very fast rates of strain, and is too time consuming at very slow rates. This difficulty is eliminated by a testing machine, developed in the Munich laboratory, provided with electronically programmed controls and automatic recorders as shown in Fig. 3. Conventional testing machines are built in such a way that one has to apply a given load to the test specimen, and record the corresponding deformation. With the new machine, however, one can subject the specimen to a predetermined deformation, and record the corresponding load. The built-in programmed control makes it possible to increase the deformation at a constant rate. The machine then records automatically the desired stress-strain diagram.

Fig. 4 shows examples of the results obtained by the described method for concretes of a 3000-psi average strength and loaded 56 days after casting. The deformations shown in the diagram are not purely

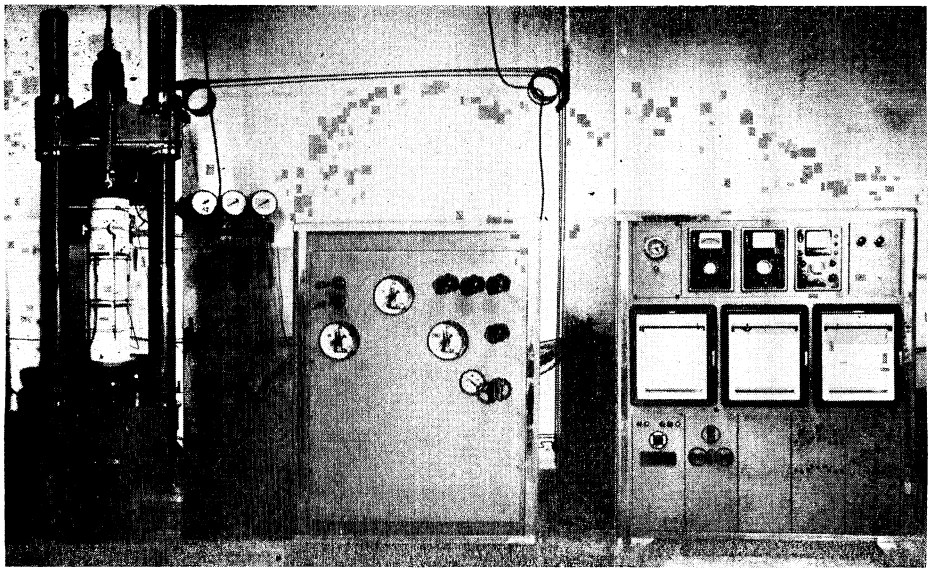

Fig. 3—Testing machine with electronically programmed control and automatic recorders

elastoplastic. The slower the rate of loading, the greater are the effects of creep and shrinkage. Naturally, there is a series of secondary factors in addition to those of strength and time, such as type of cement and cement content, grading and modulus of elasticity of aggregates, temperature, and moisture, which influence the stress-strain curve. Hence,

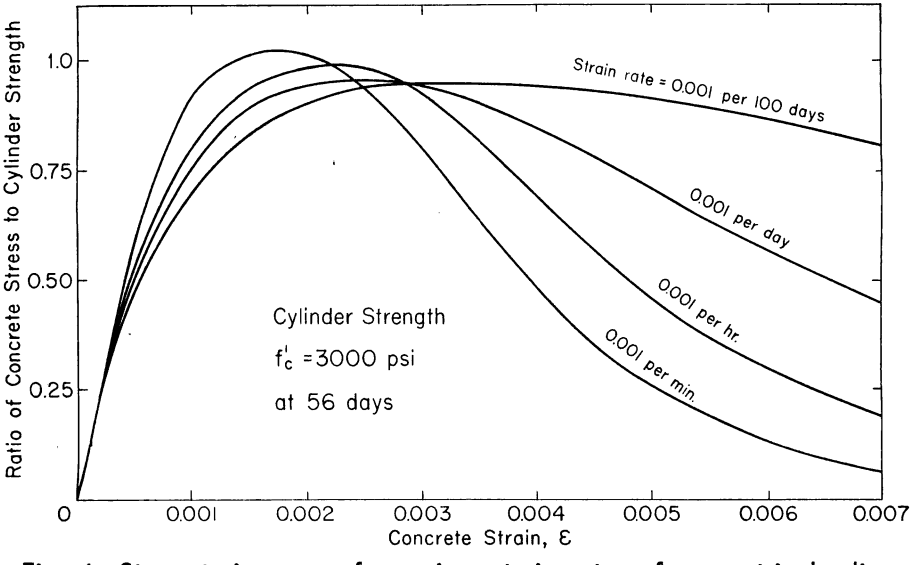

Fig. 4—Stress-strain curves for various strain rates of concentric loading

curves such as those shown in Fig. 4 may vary within certain limits. However, they will always follow the trend indicated by this diagram, which characterizes a predominating influence of time.

STRESS-STRAIN RELATIONSHIP IN FLEXURE

Seeking to establish the distribution of stresses in the concrete compression zone in flexure, it should first be considered that every "fiber" in this zone undergoes strain at a different rate. Assuming that cross sections remain plane, the rate of strain becomes proportional to the distance from the neutral axis. Furthermore, the desired stress distribution depends on the nature of load; for increasing load, on the rate at which the load is increased; for constant load, on the duration of loading.

In his paper,[5] Rasch proposes that the stress distribution in the compression zone in flexure be derived from stress-strain curves obtained from concentrically loaded prisms. How this can be done is illustrated schematically below for an example of load increasing at constant rate of strain. The stress-strain curves in Fig. 4 are used as a basis.

Fig. 5 shows schematically the derivation of the stress-strain relationship in the concrete compression zone in flexure. It is determined by the requirement that the strain of every fiber in the flexural compression zone is attained in the same interval of time, 1 hr in the chosen example. The stress corresponding to strain of 0.001 must then be selected from that stress-strain curve in Fig. 4 which corresponds to a deformation rate of 0.001 per hr. Similarly, stresses for strain of 0.003 and 0.005 are obtained from the stress-strain curves which were deter-

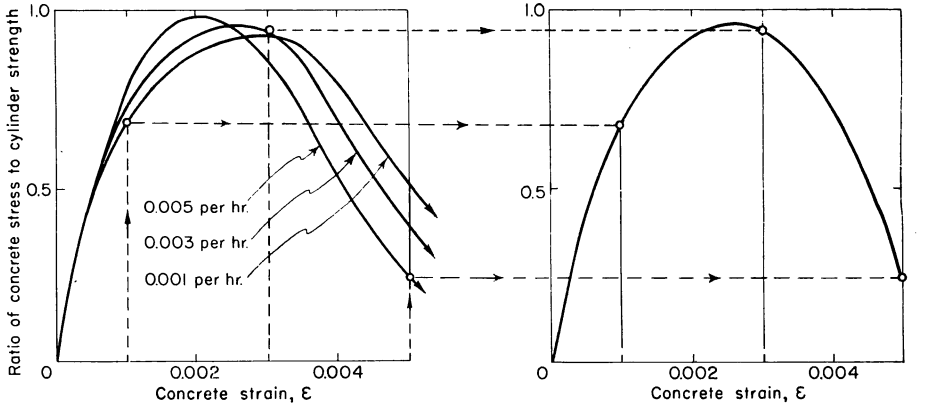

Fig. 5—Determination of stress-strain relationship in flexure (schematic only): (left) Stress-strain curves for concentric compression and various strain rates; (right) Stress-strain relationship for eccentric compression after 1 hr of loading at constant strain rates

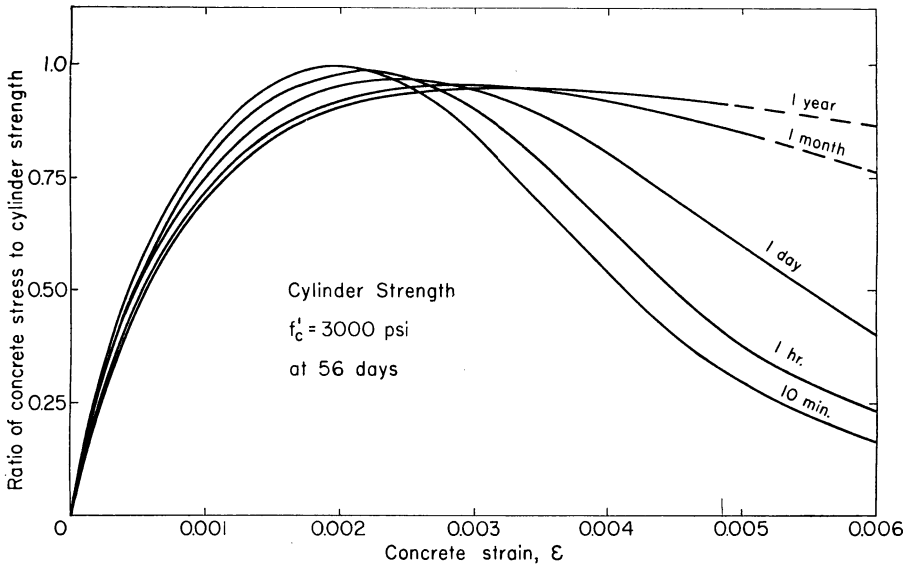

Fig. 6—Stress-strain relationships for eccentric compression after various durations of loading at constant strain rates

mined at strain rates of 0.003 and 0.005 per hr, respectively. When the stress values determined in this manner are plotted against the corresponding strains, the stress distribution for the compression zone in flexure is obtained. This applies for all loading conditions attained in 1 hr in the various fibers, under constant yet different rates of strain. The magnitude of the strain in the extreme fibers is determined by the given magnitude of load.

Several relationships are presented in Fig. 6, obtained in the above manner for various loading durations. All curves apply to the case of load increasing at constant strain rate and for an average concrete strength of 3000 psi at 56 days. These curves show clearly how important the effect of time is on the behavior of the compression zone in flexure. With decreasing rate of straining, the value of maximum stress decreases gradually. The effect of creep, however, causes a rise of the descending branch of the stress-strain curves.

The described proposal for the determination of a basic law of stress distribution pre-supposes that, for each rate of strain in the various fibers of the flexural compression zone, there appear the same stresses as in corresponding fibers of a concentrically loaded prism. This need not be strictly true in reality, because a mutual interaction of the variously deformed fibers of the compression zone in flexure may be possible due to transverse deformation. In any case the resulting errors are small — as proven by comparative tests — and do not sub-

stantially change any derived conclusions. They can be neglected in favor of a systematic study of the time factor.

COMPRESSIVE STRAIN IN EXTREME FIBERS

An important question must be answered at this stage: for an individual case, what are the values of compressive strain in the extreme fibers according to the new laws of stress distribution? This question has a simple answer: In every load test the strain in the extreme fibers is always that which will yield the required internal moment. The ultimate load is that corresponding to the maximum attainable value of the internal moment.

Fig. 7 demonstrates how the stress law can be analyzed with this aspect in mind. For a definite cross section of the compression zone in flexure and a chosen position of the neutral axis (Fig. 7 concerns a rectangular cross section and $c/d = 0.4$), the resisting moment is plotted as a function of the strain in the extreme fibers. To determine the magnitude of the internal moment, the stress block factor α and the coefficient k_2 are used to compute the magnitude and position of the concrete compressive force. These coefficients can be derived for any assumed value ε_c of the strain in extreme fibers from the stress distributions shown in Fig. 6. The curve of the relative internal

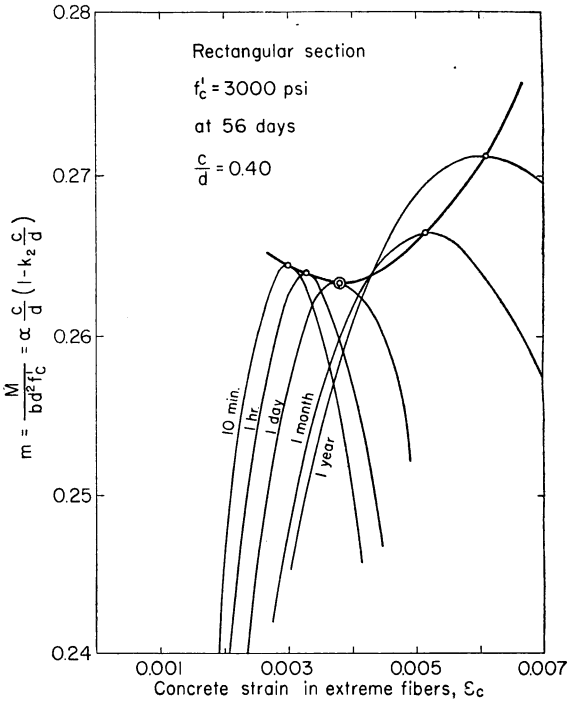

Fig. 7—Resisting moment as a function of strain and time

moment of the compression zone about the centroid of the tensile steel,

$$m = \frac{M}{bd^2 f'_c} = \alpha \frac{c}{d}\left(1 - k_2 \frac{c}{d}\right) \quad \text{.....(1)}$$

shows a clearly defined maximum in Fig. 7 for each loading duration which maximum corresponds to the ultimate moment, M_u. The corresponding strain in the extreme fibers is the ultimate strain, ε_u.

Fig. 7 further shows that the stress distributions applying to different loading durations lead to different values of ultimate moment and ultimate strain. Joining the various ultimate moments by a curve shown as a heavy line in Fig. 7, the dependence of the ultimate moment on duration of loading is seen. This curve usually shows a clear minimum. Hence, assuming that load is increased in such a manner that the rates of strain in the various fibers remain constant with time, there exists a definite duration of loading which leads to the lowest ultimate moment.

EFFECT OF POSITION OF THE NEUTRAL AXIS AND OF SHAPE OF CROSS SECTION ON ULTIMATE STRAIN

The results shown in Fig. 7 apply to one chosen position of the neutral axis only and to a rectangular cross section. When the same computations are carried out for different positions of the neutral axis and for various shapes of cross section, indications are obtained regarding

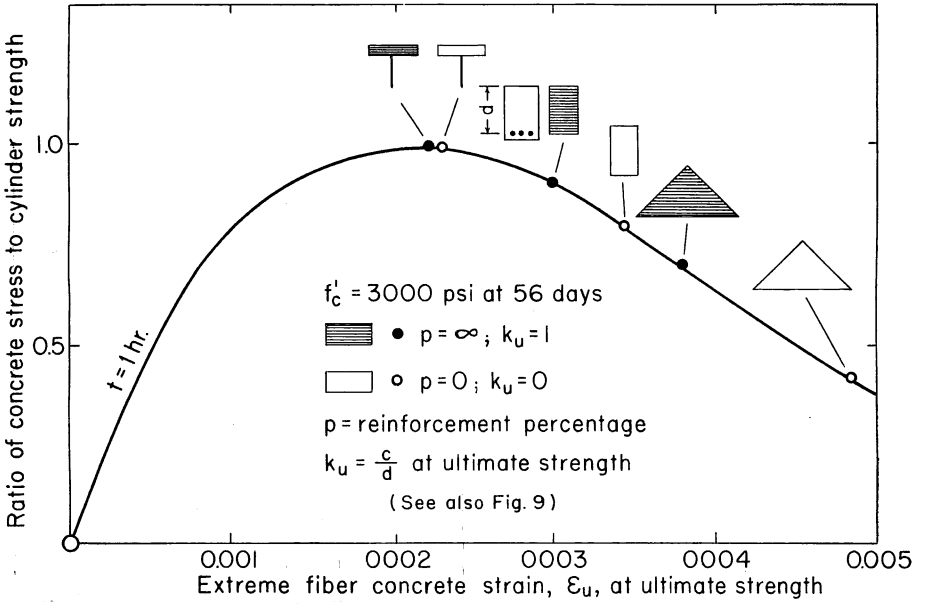

Fig. 8—Ultimate strain as a function of cross section and position of neutral axis

the degree to which the extreme fiber strain and the stress distribution at ultimate strength depend on these variables.

Examples of the results of such investigations are shown in Fig. 8. It shows extreme fiber strains at ultimate strength for several typical cross sections after 1 hr of loading and for an average concrete strength of 3000 psi at 56 days. The two mathematically extreme cases of position of the neutral axis were considered. The solid circles in the figure represent the case where the neutral axis is located at the centroid of the tension steel, the open circles denote the case when it lies at the upper edge of the cross section. In actual cases involving bending of reinforced concrete beams, the neutral axis will be between these two extreme positions. Fig. 8 shows clearly that the shape of the cross section has a decisive effect on the value of ultimate strain. For a triangular compression zone, a case which often occurs in biaxial flexure of columns, the ultimate strain is twice that for a T-beam. When the neutral axis is located at the centroid of the tension steel, this can be

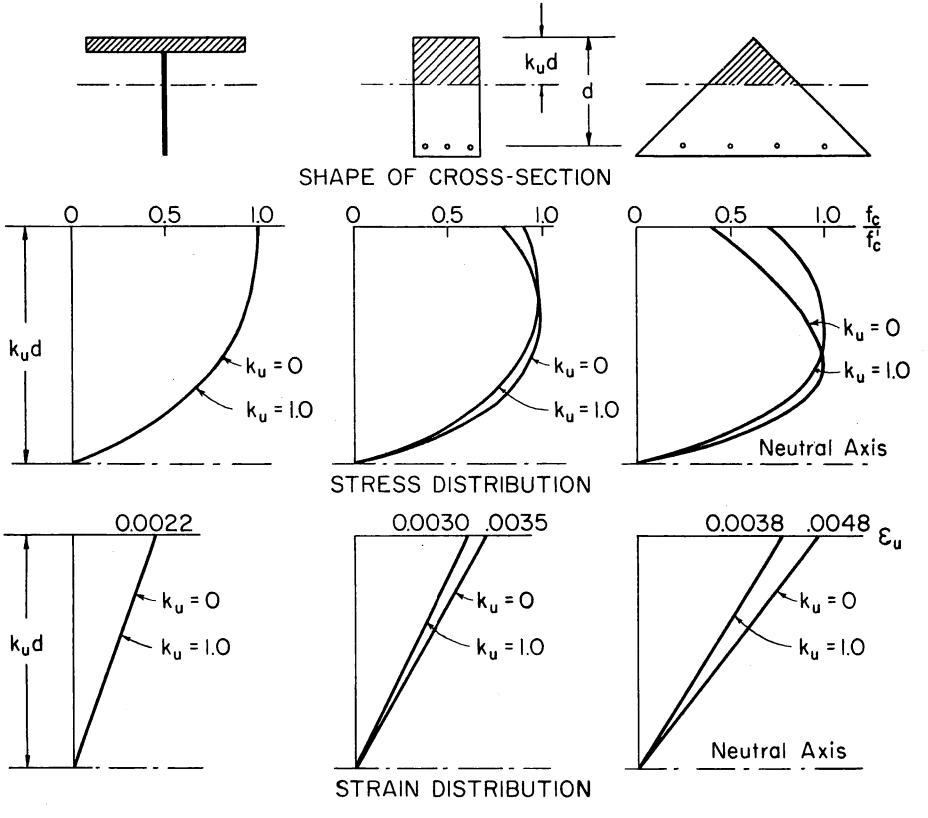

Fig. 9—Strain and stress distribution at ultimate strength after 1 hr, $f_c' = 3000$ psi at 56 days

qualitatively understood by the stress distribution shown in Fig. 9. For the idealized T cross section, most of the compression zone area is located in the upper flange, so that maximum internal moment occurs for that extreme fiber strain which gives maximum stress in the flange. For the triangular cross section, however, a major portion of the compression zone is located closer to the tension steel. Hence, maximum internal moment occurs for a relatively large extreme fiber strain giving maximum stress at some distance below the apex of the triangle. This theoretical deduction was confirmed by tests.

Fig. 8 also shows that the position of the neutral axis is of marked influence. This effect is least for T-beams and greatest for a triangular compression zone, which can be understood as follows. In an idealized T cross section, the magnitude of the lever arm of the internal forces is almost independent of the position of the neutral axis. Thus, at ultimate load, the strain in the extreme fibers is always close to that which yields the maximum internal compressive force. Conditions are different for a triangular compression zone. The magnitude of the ultimate moment is strongly affected by the length of the lever arm of the internal forces as well as by the magnitude of the internal

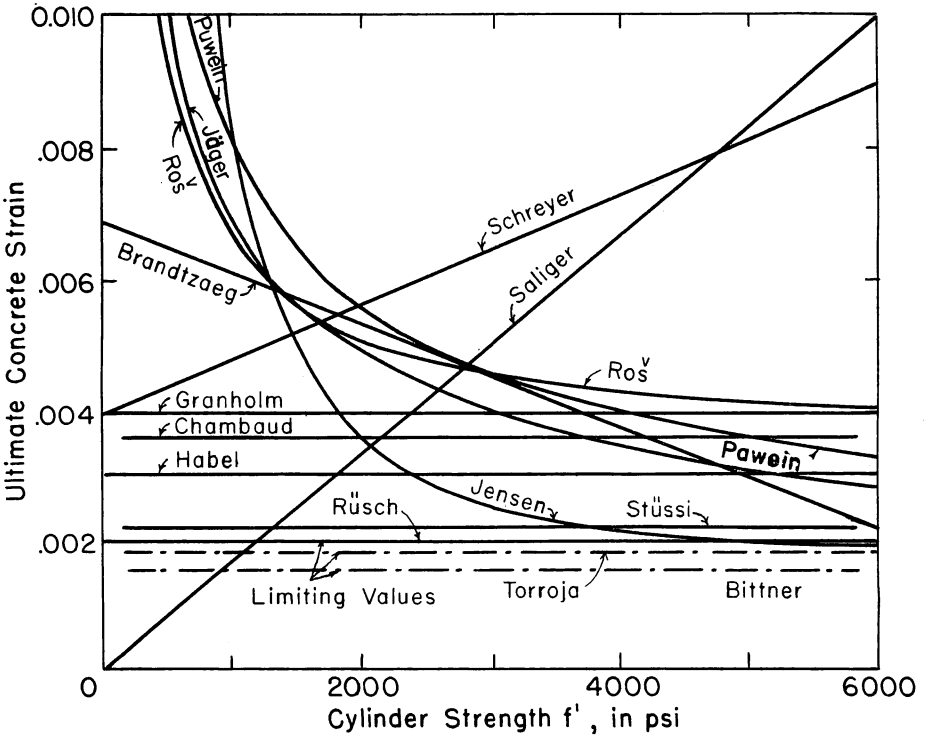

Fig. 10—Ultimate strain-concrete strength relationships

compressive force. In a rectangular cross section the position of the neutral axis still has an appreciable effect on ultimate strain.

The values reproduced in Fig. 8 and 9 apply to average concrete strength of 3000 psi and a rate of deformation at which failure takes place in 1 hr. In spite of this limitation, the value of the ultimate strain in the extreme fiber varies from about 0.0022 to 0.0048. If other concrete strengths and other rates of deformation are considered, even more pronounced differences may be expected.

A very important point is arrived at here. Most ultimate strength design theories advanced heretofore started out from the assumption that the stress distribution in the flexural compression zone, as well as the value of ultimate strain, were constant or at most dependent on concrete strength. In reality, however, these important design quantities are affected not only by concrete strength, but even to a greater degree by the *rate of loading,* the *position of the neutral axis,* and the *shape of the cross section.*

This qualitatively explains the wide divergence of the values of ultimate strain arrived at on the basis of earlier theories published by various authors, as shown in Fig. 10. It can even be argued that all these reported values, though apparently contradictory, can actually occur side-by-side. They were probably recorded under widely different conditions, and the fundamental error consisted in generalization.

EFFECT OF SUSTAINED LOADS

This discussion has so far dealt with a loading method characterized by a constant rate of strain. Even at very slow strain rates, therefore, maximum load exists only for a very short time period. This loading method is close to conditions existing in laboratory tests of structural specimens. The loading of actual structures generally takes place in a more unfavorable manner. In such structures, the load is applied relatively quickly and is then held constant.

The difference between these two types of loading is schematically illustrated in Fig. 11. The curves drawn with dashed lines correspond to loadings at constant strain rates. The rates shown correspond to failure after 1 hr, 1 day, and 3 months. The curves drawn by full lines correspond to loads applied in about 20 min and then held constant. It is seen that, for failure after a given period of time, the constant loads lead to somewhat lower failure loads than loading at constant strain rates. The investigations described below contribute to the study of these phenomena.

For some years the Munich Materials Laboratory has conducted tests of the effect of sustained load on the strength and deformation of concrete.[6,7,8] Difficulties in keeping a relatively high load constant over

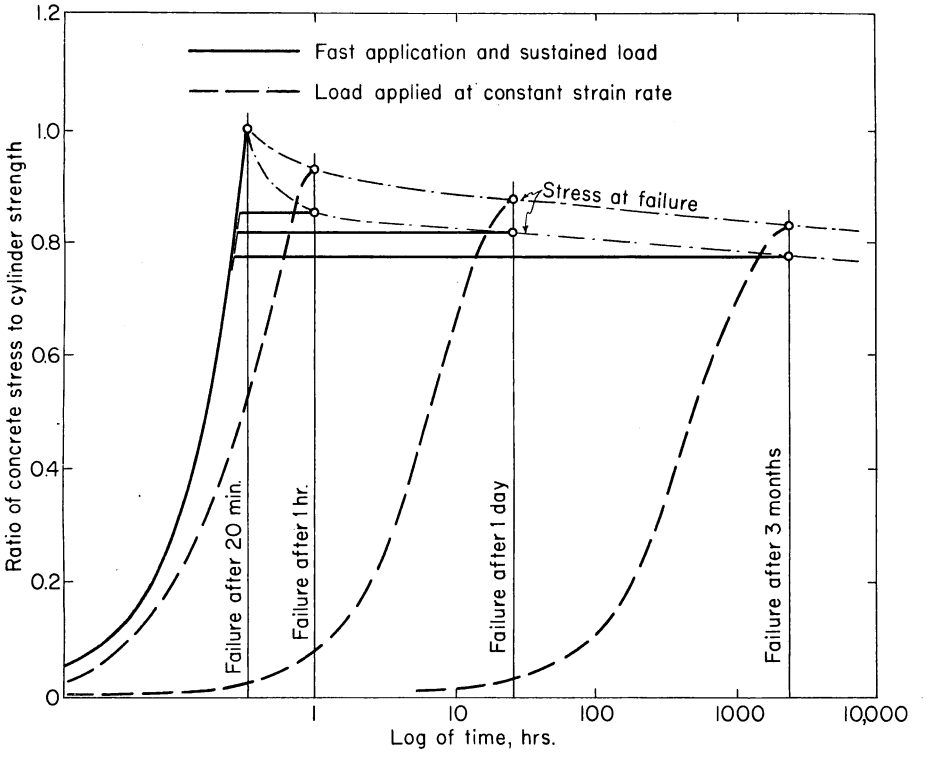

Fig. 11—Influence of type of loading on ultimate strength (schematic behavior of concentrically loaded concrete prisms)

a long period of time, even when concrete contracts under creep, were overcome by the development of a hydraulic loading arrangement such as is shown diagrammatically in Fig. 12. The piston rests on a rubber capsule which is connected to a constant pressure source. Piston leakage is eliminated, and the load can be kept constant practically without attendance. Eccentricity of loading can be varied by the hand crank arrangement shown, thus displacing the specimen laterally with respect to the force axis. Deformation was measured by mechanical strain gages.

A climate-controlled testing laboratory was used, in which a number of test specimens were subjected to load simultaneously. In these tests several identical specimens were subjected to concentric sustained load. The magnitude of load was varied for individual specimens. Its ratio to the ultimate load in a short-time test was designated as degree of loading. In this manner, the load can be determined at which the test specimen will just be able to sustain over an infinite length of time without breaking. The corresponding average compressive stress is called the sustained load strength. In addition, one observed increases in

deformation, i.e., creep under very high degrees of loading. Fig. 13 and 14 show selected results of these investigations for concentric loading and concrete of a 5000 psi average strength. The eccentricity of load was varied in other tests series.

Fig. 13 shows the influence of the degree of loading on the deformation and time elapsed up to failure. All specimens were concentrically loaded 56 days after casting. The failure in a conventional short-time test occurs in about 20 min at an ultimate strain of about 0.0025. For specimens subjected to a sustained load with degree of loading less than one, two families of curves with different characteristics are obtained. As long as the degree of loading is higher than that corresponding to the sustained load strength, the deformations eventually increase rapidly and lead to failure. For loading below the sustained load strength, the deformation curves become stabilized and approach limiting values of strain.

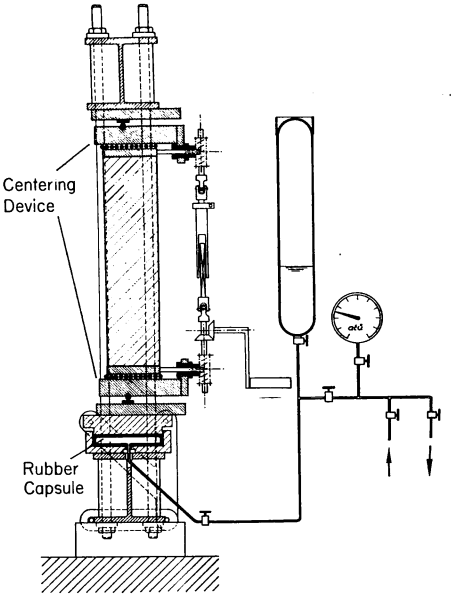

Fig. 12—Testing arrangement for sustained load tests

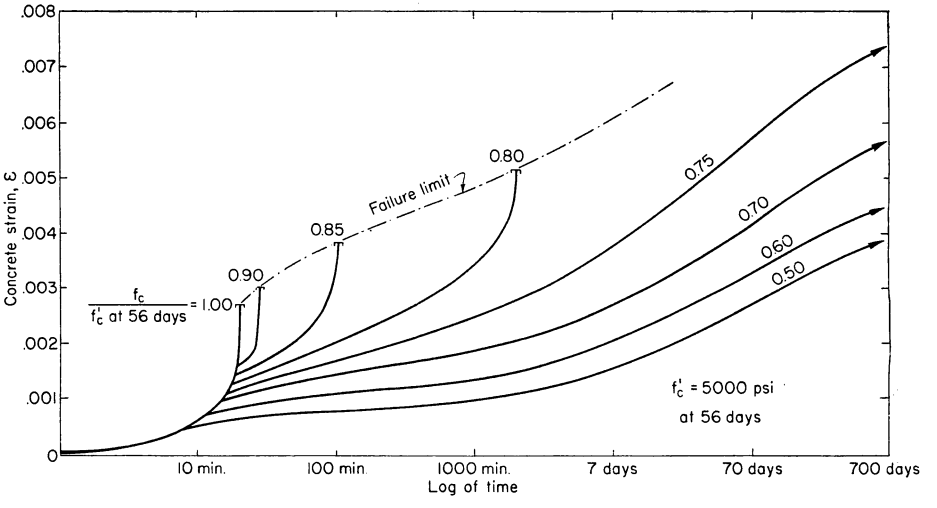

Fig. 13—Strains under sustained load applied at concrete age 56 days (concentric loading of prisms at 56 days)

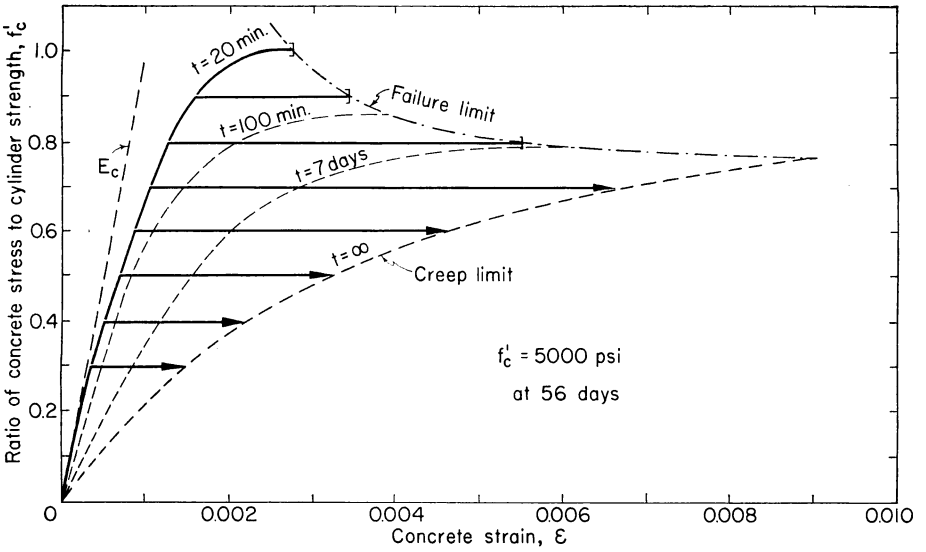

Fig. 14—Influence of load intensity and duration on concrete strain

The same results are given in Fig. 14 in terms of curves for applied load versus strain with time after loading at an age of 56 days as a parameter. It can be expected that the limiting line on the left of the diagram will become close to a straight line for extremely short durations of loading, until finally it will coincide with the elastic straight line relationship denoted E_c in the figure. On the lower right the diagram is limited by the creep deformations corresponding to an infinite duration of loading. At the top, the diagram is limited by the failure line, which shows decreasing strength for increasing load duration. The two parameter curves shown between these limits correspond to conditions after 100 min and after 7 days, respectively. The limiting lines of the diagram described above, enclose all possible relationships between stress and strain.

The Munich tests have shown that sustained load strength of a concentrically loaded concrete specimen amounts to at least 75 percent, and on the average to about 80 percent of the strength determined in a short-time test. The short-time strength is then defined as the strength of an identically cast and identically old specimen, which remains without load and is tested in a standard short-time test of about 10 min duration at the time when the twin specimen under sustained load has collapsed. This short-time strength depends on age and storage conditions and is usually greater than the strength at the time of loading which is used as a basis in Fig. 13 and 14.

The ratio of sustained-load strength to short-time strength is, according to our evidence, independent of concrete strength. In accordance with the chosen definitions it is also fairly independent of concrete age at

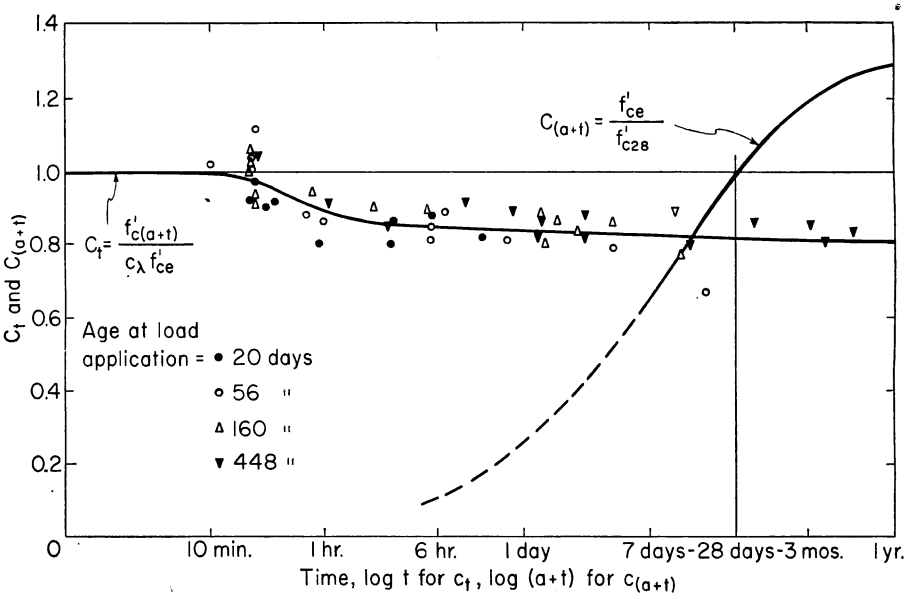

Fig. 15—Effects of time on strength

application of sustained load. However, since short-time strength increases with time after casting, the time elapsed until failure still has a pronounced effect on the absolute value of the sustained-load strength.

Concrete loaded shortly after casting is subjected to two different effects. The strength reduction caused by sustained load is counteracted by the strength increase with time. As the strength reduction due to sustained loading is particularly pronounced immediately following application of load, failure of a young concrete constitutes a danger only during the first days after load application. The effect of additional hardening becomes predominant thereafter. In contrast to this, for a very old concrete which has reached practically its full strength before it is loaded, failure under sustained load may occur after very long periods of loading. This effect of age at loading can be approximately expressed by the following relation, set up on the basis of the test findings shown in Fig. 15 and 16. The strength of a concrete failing under sustained load at the

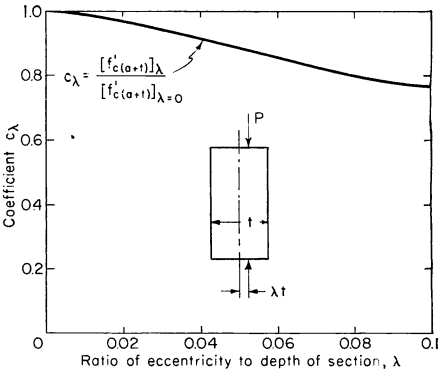

Fig. 16—Effect of eccentricity on strength

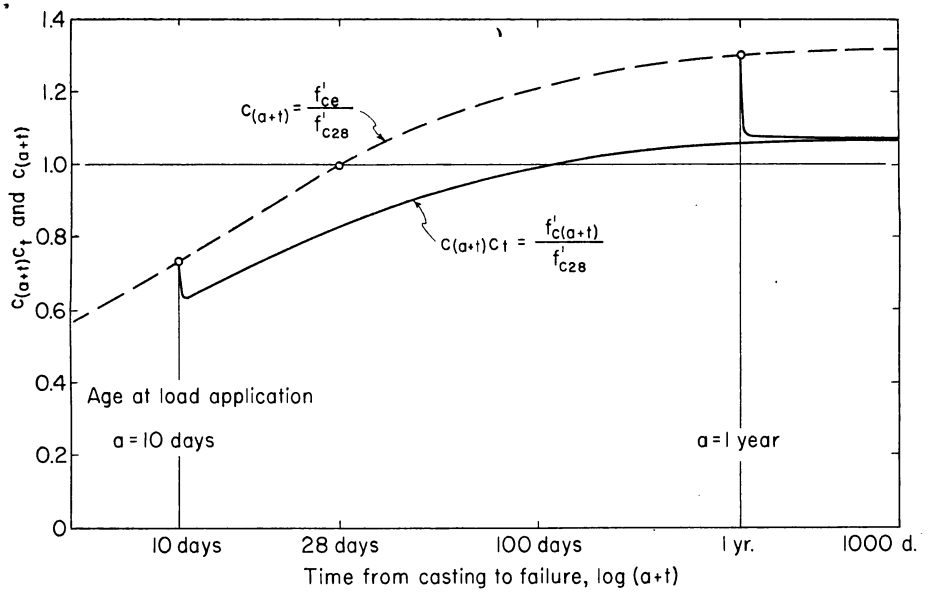

Fig. 17—Effect of age at load application on sustained load strength

time t days after loading at an age of a days is:

$$f'_{c(a+t)} = f'_{c28}\, c_{(a+t)}\, c_t\, c_\lambda = f'_{ce}\, c_t\, c_\lambda \quad \ldots\ldots (2)$$

in which f'_{c28} represents the concrete strength at the age of 28 days; a denotes the age of concrete at the beginning of sustained load application; t is duration of load after the full load (applied in a period of 20 min) has been reached; f'_{ce} is the short-time concrete strength at an age of $(a + t)$ days; and λ is the relative eccentricity of the load $\lambda = e/t$. In this manner, the effects of continued hardening and of eccentricity of load are expressed by the coefficients $c_{(a+t)}$ and c_λ, which can be obtained directly from experimental data. The values of the coefficient c_t, expressing the influence of the sustained load, were derived by means of Eq. (2) from sustained load test data. The curve to the right in Fig. 15 shows the effect, $c_{(a+t)}$, of continued curing on short-time strength for a concrete with a 28-day strength of 4300 psi. The flat curve beginning to the left expresses the effect of sustained loading, c_t, and was determined for sustained loadings applied from 20 to 448 days after casting. Fig. 16 shows the effect, c_λ, of eccentricity on the average compressive stress at failure. The tests indicated that c_λ is independent of the duration of loading. Hence, values determined with particular care in short-time tests were used to develop the relationship shown in Fig. 16.

Fig. 17 reproduces results derived from Eq. (2) for two groups of concentrically loaded test specimens ($\lambda = 0$; $c_\lambda = 1.0$), loaded at ages

of 10 days and 1 year. The selected logarithmic scale provides a good general trend, but does not reveal the details of strength changes occurring immediately after loading. Therefore, the same values were plotted in Fig. 18 on a larger time scale and as a function of duration of load. This diagram reveals clearly that the lowest strength is attained in the young concrete after a loading duration of 6 hr, while no minimum is apparent for old concrete even after a loading duration of several years.

The interrelationship between the sustained load strength, the age of concrete at application of load, the duration of loading, and the eccentricity of the applied load has been discussed. The question of deformation existing at failure is a more difficult problem. The failure does not occur suddenly, but it is a result of a gradual destruction of the internal structure of the material accompanied by a rapid increase of the deformation as shown in Fig. 13. Hence, it is difficult to give a reliable value for the deformation at ultimate strength. The test values vary within a wide range and apply to a stage in which the deformations already have reached values that are excessive in terms of practical usefulness.

Under these circumstances it is suitable for design purposes to consider a state of deformation which precedes failure. This can be done in various ways, for example, one could consider the deformation just at the onset of its rapid increase, indicating that failure is imminent. The writer feels that a suitable choice of deformation is that which exists at one-half of the loading duration to failure in sustained load

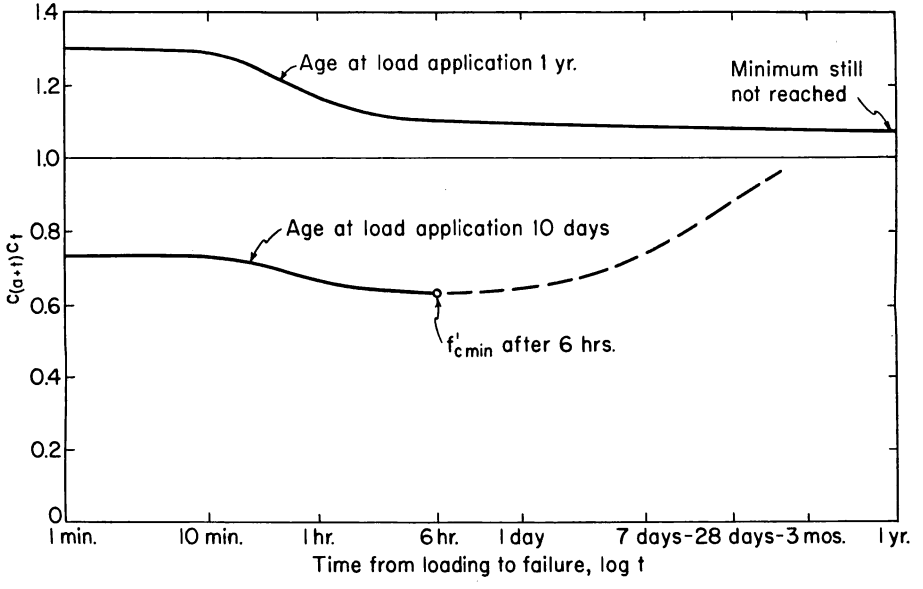

Fig. 18—Influence of time on strength under sustained concentric load

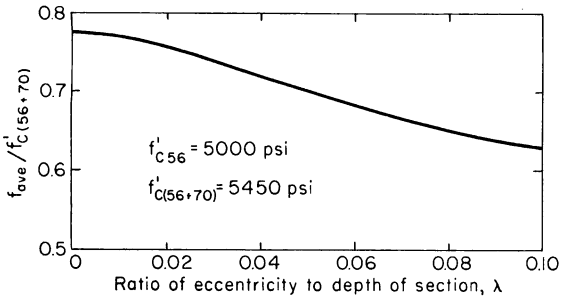

Fig. 19 — Average stress at ultimate eccentric sustained load

tests. As another possibility deformations to be used in design could be obtained by a test, in which the degree of loading is below the sustained ultimate strength, say 90 per cent.

It is not intended to discuss the advantages and disadvantages of such possibilities here. This would be worthwhile only if sufficient experimental data were available, so that the relative merits of the various methods could be evaluated. In the following, therefore, only the basic concepts of the new approach will be presented. The principal reason for selecting the deformation at one-half the time to failure is that sufficient experimental data were available from sustained load tests of 70 days duration between loading and failure.

Fig. 19 and 20 reproduce some results of the eccentric sustained load test series of concrete prisms which results are used as a basis for the present formulation of flexural theory. Fig. 19 shows the relation-

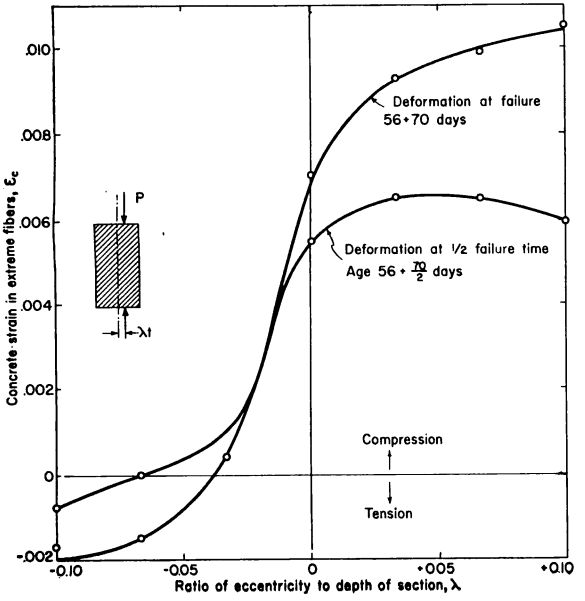

Fig. 20 — Strain in extreme fibers under sustained load

ship between load eccentricity and the average compressive stress causing failure after 70 days under sustained load. The load was applied 56 days after casting. The corresponding edge deformations are shown in Fig. 20 for load duration of 35 and 70 days, that is, for half the failure time and the complete time to failure.

In Fig. 19 and Fig. 20 the deformation developing at both edges and the corresponding average value of the stresses leading to failure after a duration of loading of 70 days can be read off for variable eccentricity. It was attempted to derive a stress-strain relationship which would correlate these test results. To this end a stress diagram limited by the two edge deformations was drawn for each value of eccentricity. The area and center of gravity of the diagram must conform to the measured values. As a first attempt diagrams were used whose upper boundaries were parabolic. The boundary lines shown in Fig. 21 fit rather well into a continuous stress-strain envelope. By trial and error better curves can be found as more test results become available. The remaining deviations will be tolerable and to a large extent attributable to unavoidable scatter of test results.

Fig. 22 presents the derived stress-strain envelope which applies for one-half the load duration in tests carried out on concrete which failed after 70 days' duration of sustained load, applied 56 days after casting.

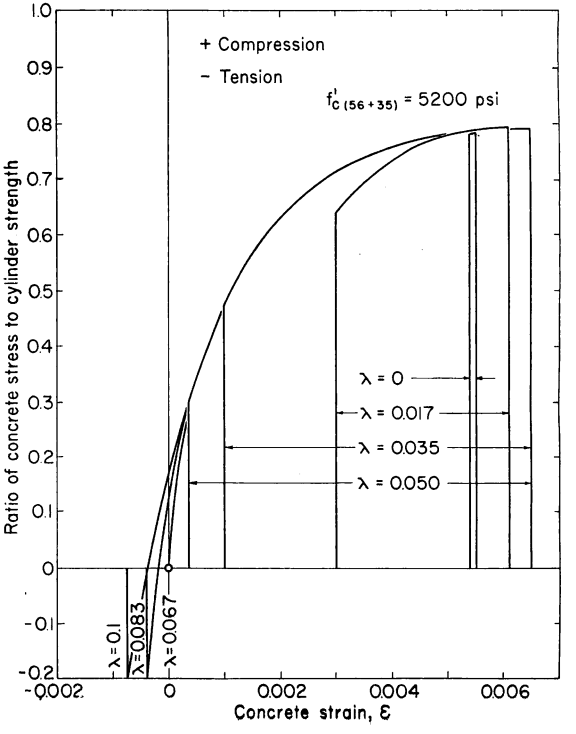

Fig. 21 — Stress-strain relationship from eccentric load tests at one-half failure time

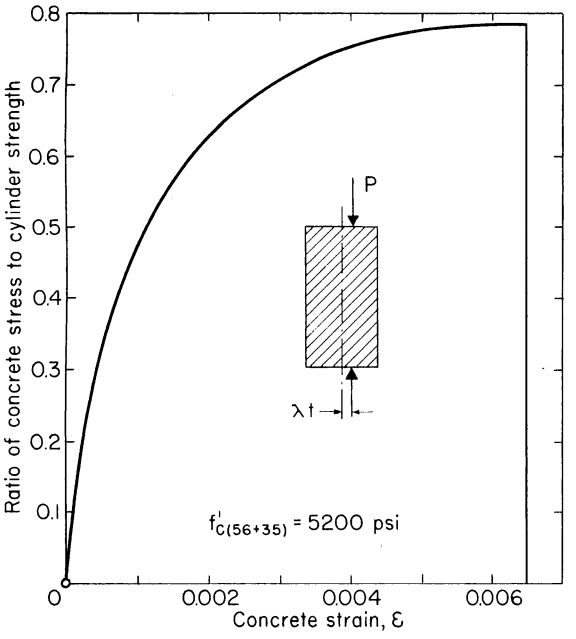

Fig. 22 — Probable stress-strain relationship from sustained load

This curve establishes another basic law of stress distribution which permits study of strength in the compression zone of structural members as a function of shape of cross section and position of the neutral axis. This can be carried out in the same manner as described in the present paper for stress-strain curves derived for constant rates of deformation.

The curve of Fig. 22 applies only to an age at loading of 56 days and a duration to failure under sustained load of 70 days. In the same manner one can, of course, by further experiments find curves which would apply to other ages, loadings, and load durations.

PRESENTATION OF THE RESULTS IN A DIAGRAM

The author suggested in 1950 [9] plotted the values required in ultimate strength design of rectangular cross sections as a function of the reduced moment of the internal concrete compressive force about the centroid of tensile reinforcement: $m_u = M_u/bd^2 f_c'$. Two coefficients are plotted as ordinates which define values at ultimate strength of the position of the neutral axis ($k_u = c/d$), the lever arm of the internal forces ($j_u = j_u d/d$), and also the strain (ε_{su}) in tensile reinforcement.

Fig. 23 shows the values of these coefficients at ultimate strength for a case of rectangular cross section and average concrete strength of 5000 psi at 400 days for constant strain rate, and at 56 days for sustained load. The diagram also takes into account effects of time. Several cases of loading at constant rate of strain were considered, the time elapsing to

failure being 10 min to 1 year. In addition, the case of sustained load applied at the age of 56 days and held constant to failure at 70 days was considered. The following comments will serve to explain the diagram:

(a) Because the values $m_u = M_u/bd^2f_c' = (M_o + P_o\ e_s)/bd^2f_c'$ were selected as abscissae,* this diagram applies to the case of pure flexure as well as to the case of combined flexure and compression. In general, low m_u values correspond to pure bending, and high m_u values to combined flexure and compression.

(b) The lowest coefficient in the diagram for the lever arm of the internal forces is $j_u = 0.50$. The resultant of the internal compressive stresses then is at the center of the cross section, that is, the case is one of a concentrically loaded column.

(c) The coefficients k_u and j_u, which determine the position of the neutral axis and the lever arm of the internal forces, are least affected by duration of loading. The coefficient k_u increases with increasing duration of loading, since the strength reduction due to time is compensated for by a lowering of the neutral axis. This leads to a reduction of the lever arm of the internal forces, expressed by a reduction of the coefficient j_u.

(d) The strain in tensile reinforcement, ε_{su}, is most strongly affected by duration of loading.

CONCLUDING REMARKS

This paper presents only an outline of a new flexural theory. The author is well aware that this work has not yet come to a decisive conclusion, and that the proposed design method does not constitute a completed solution. Thus, for example, there may be divided opinions as to the selection of the loading state from which the deformations forming the basis for sustained load design are to be determined.

Naturally it is unthinkable that practical design should involve the effect of duration of loading in detail. Not only would such a procedure be much too laborious, but it must also be admitted that in most cases it cannot be foreseen at all what service loads a structure will actually be called upon to carry during its lifetime.

Under these circumstances one is forced to start out from the least favorable conditions which can normally occur. The diagrams shown above permit us to realize clearly that these least favorable conditions occur under long-time action of a constant load.

The safety of reinforced concrete structures is generally related to their strength at 28 days. According to the reasoning followed in this paper, failure under sustained load can occur in young concrete only during the first few days, as long as ordinary portland cement is used. Furthermore, the case of young concrete being subjected to high loads is possible in most structures due to so-called construction loads.

*M_u is internal moment of concrete force about centroid of tensile reinforcement at ultimate strength; M_o is moment of external forces about centroid of section; P_o is external axial force acting in centroid of section; and e_s is distance between tensile reinforcement and section centroid.

Therefore, the requirement to design all structural units for a low age at loading, such as 28 days, is not unreasonable.

In this manner, it appears possible to replace the families of curves in Fig. 23 by a new design diagram, which presents only one curve for each of the three quantities needed in design, k_u, j_u, and ε_{su}. Tests which could be used in establishing these curves are lacking at present. However, by interpolating tests for other ages at loading, it is possible to estimate the probable shape of these curves. This is presented in

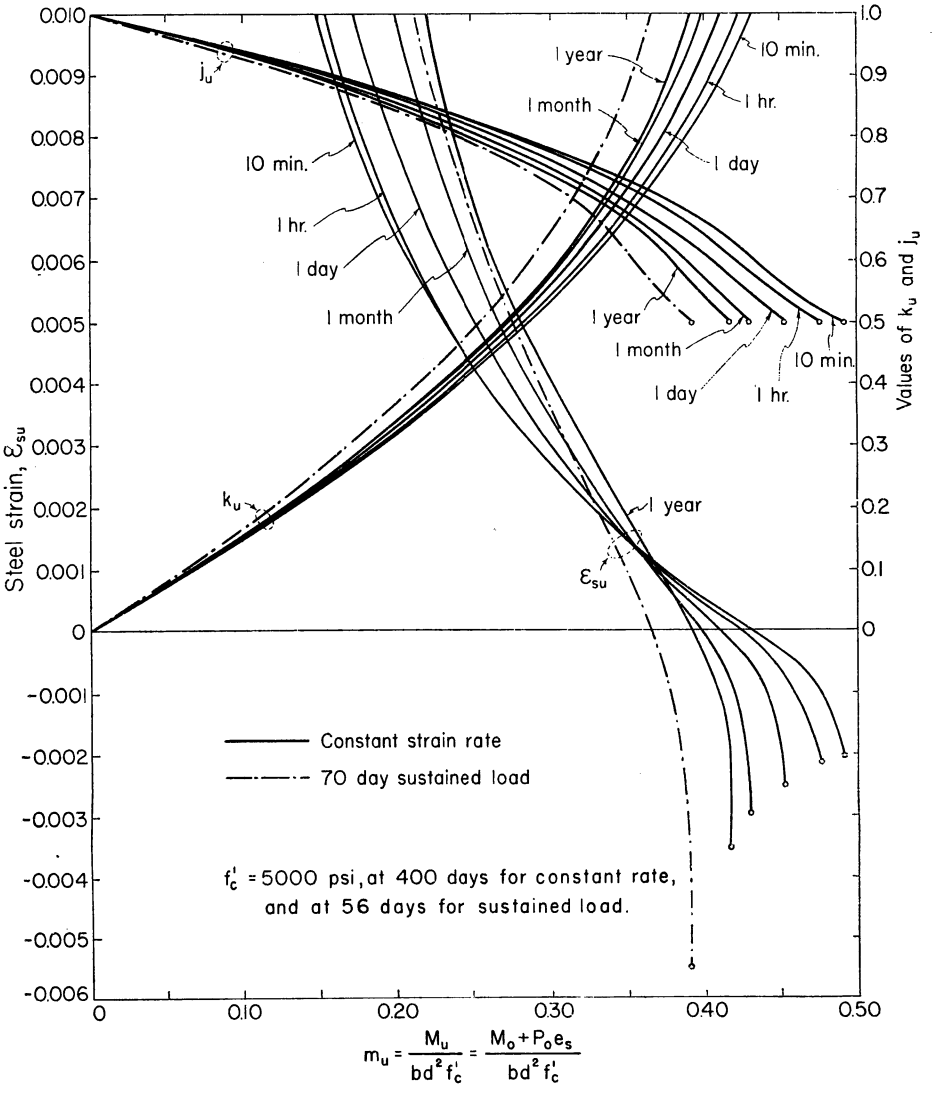

Fig. 23—Values of k, j, and ε_s at ultimate strength of rectangular cross sections

Fig. 24, although only for an average concrete strength of 4300 psi at 28 days. The final design chart should contain the three curves for each of several concrete qualities. The j_u curves will probably be so close together that they can be replaced by a single curve.

Such a diagram appears to offer the best opportunity to summarize in a simple form all the results of the theory of flexure developed here. Naturally, there are many other methods of presenting the quantities needed in everyday design, such as diagrams, tables, and simplified empirical formulas.

The advantage of a design chart of the type shown in Fig. 24 lies in its general scope of application. It embraces the entire range of

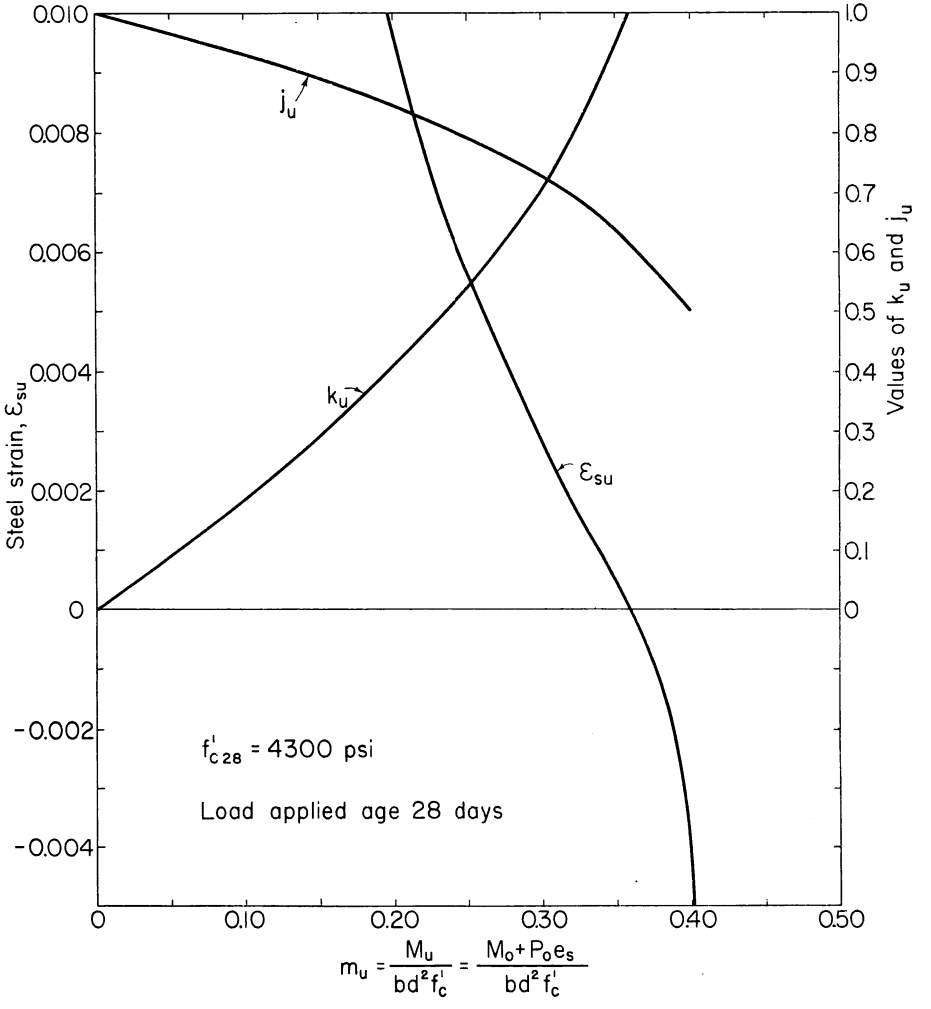

Fig. 24—Probable ultimate strength design chart for sustained load on rectangular members

stress conditions from pure bending to concentric compression. It can be used for all concrete strengths and steel qualities and applies to reinforced concrete as well as prestressed concrete. The diagram applies, however, only to rectangular cross sections, although similar diagrams can be plotted for other cross sectional shapes. The general applicability of such a diagram is illustrated in the appendix.

REFERENCES

1. Hognestad, E., "A Study of Combined Bending and Axial Load in Reinforced Concrete Members," *Bulletin* No. 399, University of Illinois Engineering Experiment Station, 1951, 128 pp.

2. Hognestad, E.; Hanson, N. W.; and McHenry, D., "Concrete Stress Distribution in Ultimate Strength Design," ACI JOURNAL, V. 27, No. 4, Dec. 1955 (*Proceedings* V. 52), pp. 455-479.

3. Moenaert, P., "Étude Expérimentale de la Rupture d'une Pièce Longue en Béton Armé Sollicitée par Flexion Plane Composée non Déviée," (Experimental Study of Failure in Reinforced Concrete Members Subject to Combined Axial Load and Flexure), Imprimerie G.I.C., Brussels, 1953, 162 pp.

4. Rüsch, H., "Versuche zur Festigkeit der Biegedruckzone," (Tests on the Strength of the Flexural Compression Zone), *Bulletin* No. 120, *Deutscher Ausschu für Stahlbetonbau* (Berlin), 1955, 94 pp.

5. Rasch, C., "Stress-Strain Diagrams of Concrete Obtained by Constant Rates of Strain," RILEM Symposium on the Influence of Time on the Strength and Deformation of Concrete, Munich, 1958.

6. Rüsch, H., "Der Einfluss der Zeit auf Festigkeit und Verformung," (The Influence of Time on Strength and Deformation), *Final Report,* Fourth Congress, International Association for Bridge and Structural Engineering, Cambridge and London, 1952.

7. Rüsch, H., "Versuche zur Bestimmung des Einflusses der Zeit auf Festigkeit und Verformung," (Experimental Determination of the Effect of the Duration of Loading on Strength and Deformation), *Final Report,* Fifth Congress, International Association for Bridge and Structural Engineering, Portugal, 1957.

8. Rüsch, H.; Sell, R.; Rasch, C.; and Stöckl, S., "Investigations on the Strength of Concrete under Sustained Load," RILEM Symposium on the Influence of Time on the Strength and Deformation of Concrete, Munich, 1958.

9. Rüsch, H., "Bruchlast und Bruchsicherheitsnachweis bei Biegungsbeanspruchung von Stahlbeton unter besonderer Berücksichtigung der Vorspannung," (Strength and Safety in Bending of Reinforced Concrete with Consideration of Prestressing), *Beton und Stahlbeton* (Berlin), V. 45, No. 9, 1950, pp. 215-220.

APPENDIX — DESIGN EXAMPLES

The four examples below apply to a rectangular cross section with dimensions as shown in Fig. A-1. The quantities k_u, j_u, ε_{su} needed in design are taken from the design diagram in Fig. 24. It should be emphasized again that the internal and external forces given in the examples of this appendix correspond to ultimate strength.

Example No. 1

Design load:	Pure bending; $M_o = 2620$ in.-kips
Material:	Reinforced concrete; $f_c' = 4300$ psi; cold worked deformed bars (see Fig. A-1)

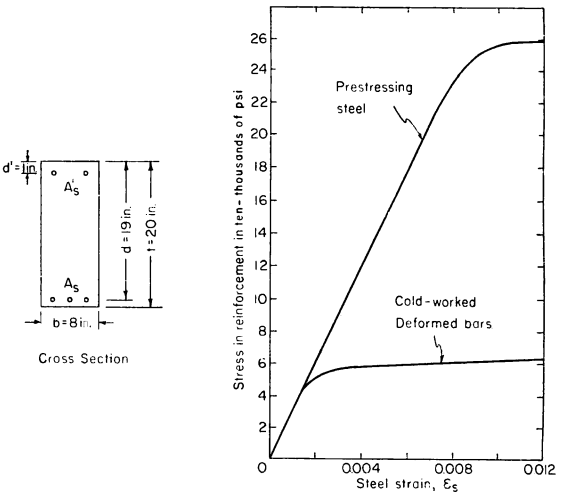

Fig. A-1—Design cross section and stress-strain curves for reinforcing steel

Relative moment: $m_u = \dfrac{M_o}{bd^2 f_c'} = \dfrac{2620}{9 \times 19^2 \times 4.3} = \dfrac{2620}{12{,}420} = 0.211$

Internal moment arm: $j_u d = 0.832 \times 19 = 15.8$ in.

Steel stress: for $\varepsilon_{su} = 0.0085$, $f_{su} = 59.8$ ksi (steel yielding)

A_s required: $\dfrac{M_u}{j_u d\, f_{su}} = \dfrac{2620}{15.8 \times 59.8} = 2.77$ sq in.

Example No. 2a

Design load: Bending and axial load acting at section centroid; $M_o = 2620$ in.-kips, $P_o = 156$ kips

Material: Same as in Example 1

Moment about tensile reinforcement: $M_u = M_o + P_o\,(d - t/2) = 2620 + 156\,(19 - 10)$
$= 4024$ in.-kips

Relative moment: $m_u = \dfrac{4024}{12{,}420} = 0.324$

Internal moment arm: $j_u d = 0.690 \times 19 = 13.1$ in.

Steel stress: for $\varepsilon_{su} = 0.00165$, $f_{su} = 46.5$ ksi

A_s required: $\dfrac{1}{f_{su}}\left(\dfrac{M_u}{j_u d} - P_o\right) = \dfrac{1}{46.5}\left(\dfrac{4024}{13.1} - 156\right) = 3.25$ sq in.

Example No. 2b

Design load: Bending and axial load acting at section centroid; $M_o = 3500$ in.-kips, $P_o = 156$ kips

Material: Same as Example 1, plus compressive reinforcement: $A_s' = 0.80$ sq in., $d' = 1$ in.

Moment about tensile reinforcement: $= 3500 + 156\,(19 - 10) = 4900$ in.-kips

Estimated position of neutral axis: $k_u = 0.80$; $c = k_u d = 0.80 \times 19 = 15.2$ in.

Tensile steel strain:	$\varepsilon_{su} = 0.00162$
Compressive steel strain:	$\varepsilon'_{su} = \varepsilon_{su}\frac{c-d'}{d-c} = 0.00162\frac{15.2-1}{19-15.2} = 0.0060$
Moment resisted by compressive reinforcement:	$= A_s' f'_{su}\ (d-d') = 0.8 \times 58.6 \times 18 = 844$ in.-kips
Moment resisted by concrete:	$M_u = 4900 - 844 = 4056$ in.-kips
Relative moment:	$m_u = \frac{4056}{12{,}420} = 0.327$
New position of neutral axis:	$k_u = 0.813$ (0.80 estimated k_u is all right)
Internal moment arm:	$j_u d = 0.685 \times 19 = 13.0$ in.
Stress in tensile reinforcement:	for $\varepsilon_{su} = 0.0015$, $f_{su} = 45.0$ ksi
A_s required:	$\frac{1}{f_{su}}\left(\frac{M_u}{j_u d} - P_o\right) + A_s'\frac{f'_{su}}{f_{su}}$ $= \frac{1}{45.0}\left(\frac{4056}{13.0} - 156\right) + 0.80\frac{58.6}{45.0}$ $= 4.51$ sq in.

Example No. 3

Design load:	Pure bending; $M_o = 3500$ in.-kips
Material:	Prestressed concrete, bonded, $f_c' = 4300$ psi; prestressing steel, see Fig. A-1
Relative moment:	$m_u = \frac{3500}{12{,}420} = 0.282$
Internal moment arm:	$j_u d = 0.753 \times 19 = 14.3$ in.
Strain at level of reinforcement:	$\varepsilon_{cu} = 0.0037$
Strain in reinforcement due to effective prestress:	$\varepsilon_{se} = 0.0040$
Total strain in reinforcement:	$\varepsilon_{su} = \varepsilon_{cu} + \varepsilon_{se} = 0.0077$
Steel stress:	$f_{su} = 227$ ksi
A_s required:	$\frac{M_u}{j_u d\, f_{su}} = \frac{3500}{14.3 \times 227} = 1.08$ sq in.

Received by the Institute Apr. 25, 1960. Title No. 57-1 is a part of copyrighted Journal of the American Concrete Institute, V. 32, No. 1, July 1960 (Proceedings V. 57). Separate prints are available at 60 cents each.

American Concrete Institute, P. O. Box 4754, Redford Station, Detroit 19, Mich.

Discussion of this paper should reach ACI headquarters in triplicate by Oct. 1, 1960, for publication in March 1961 JOURNAL.